Accepted Manuscript

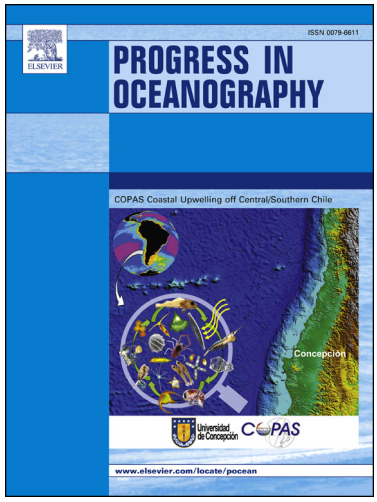

Decrease in diatom palatability contributes to bloom formation in the Western English Channel

L. Polimene, A. Mitra, S.F. Sailley, S. Ciavatta, C.E. Widdicombe, A. Atkinson, J.I. Allen

PII: S0079-6611(15)00093-2
DOI: http://dx.doi.org/10.1016/j.pocean.2015.04.026
Reference: PROOCE 1580

To appear in: *Progress in Oceanography*

Received Date: 28 June 2014
Revised Date: 13 October 2014
Accepted Date: 22 April 2015

Please cite this article as: Polimene, L., Mitra, A., Sailley, S.F., Ciavatta, S., Widdicombe, C.E., Atkinson, A., Allen, J.I., Decrease in diatom palatability contributes to bloom formation in the Western English Channel, *Progress in Oceanography* (2015), doi: http://dx.doi.org/10.1016/j.pocean.2015.04.026

Decrease in diatom palatability contributes to bloom formation in the Western English Channel

L. Polimene*[1], A. Mitra[2], SF Sailley[1], S. Ciavatta[1], CE Widdicombe[1], A. Atkinson[1], JI Allen[1]

[1]Plymouth Marine Laboratory

[2] Centre for Sustainable Aquatic Research (CSAR), Swansea University, Swansea SA2 8PP, UK

ABSTRACT: The aim of this paper is to investigate the role of phytoplankton nutritional status in the formation of the spring bloom regularly observed at the station L4 in the Western English Channel. Using a modelling approach, we tested the hypothesis that the increase in light from winter to spring induces a decrease in diatom nutritional status (i.e. an increase in the C:N and C:P ratios), thereby reducing their palatability and allowing them to bloom. To this end, a formulation describing the Stoichiometric Modulation of Predation (SMP) has been implemented in a simplified version of the European Regional Seas Ecosystem Model (ERSEM). The model was coupled with the General Ocean Turbulence Model (GOTM), implemented at the station L4 and run for ten years (2000-2009). Simulated carbon to nutrient ratios in diatoms were analysed in relation to microzooplankton biomass, grazing and assimilation efficiency. The model reproduced *in situ* data evolutions and showed the importance of microzooplankton grazing in controlling the early onset of the bloom. Simulation results supported our hypothesis and provided a conceptual model explaining the formation of the diatom spring bloom in the investigated area. However, additional data describing the microzooplankton grazing impact and the variation of carbon to nutrient ratios inside phytoplanktonic cells are required to further validate the proposed mechanisms.

*Corresponding author: luca@pml.ac.uk

KEY WORDS: diatom bloom, phytoplankton stoichiometry, zooplankton assimilation efficiency, Station L4

INTRODUCTION

Phytoplankton blooms are important events triggering a series of processes and trophic interactions which impact the whole marine ecosystem, from biogeochemical cycles to secondary production and fisheries (Legendre, 1990; Irigoien et al. 2005). These blooms manifest as a dramatic increase in the phytoplankton standing stock over a relatively short period of time.

Some studies have emphasised the role of the physical environment in creating the conditions required for a bloom (Huisman et al., 1999; Taylor and Ferrari 2011; Smyth et al, 2014) while others have suggested that biotic factors such as grazing and phytoplankton physiology could also play a critical role (Irigoien et al., 2005; Mitra and Flynn 2006). However, a conceptual model integrating the contribution of abiotic and biotic elements to the formation and evolution of a phytoplanktonic bloom is still lacking.

Recently, Smyth et al (2014) suggested that the air-sea heat flux play a crucial role in triggering phytoplankton blooms in the Western English Channel. By analysing historical time series data, at station L4 south of Plymouth (http://www.westernchannelobservatory.org.uk), these authors found that the beginning of the phytoplankton blooms regularly (on average by 30 days) follows the inversion of the net heat flux (NHF) into the ocean from negative to positive. Positive NHF (i.e., heat flux from atmosphere to ocean) decreases the turbulence and hence vertical mixing. This leads to an increase in the residence time of phytoplankton in the euphotic zone allowing some phytoplanktonic groups (such as diatoms) to escape grazing control and form blooms. In contrast, phytoplankton stocks are likely to be controlled by microzooplankton during winter when the NHF is negative (i.e., heat flux from ocean to atmosphere) and increase in vertical mixing prevents an adequate light exposure for growth.

All the above mentioned physical factors not only affect directly the timing and amplitude of the bloom but also have the potential to modulate biotic responses which facilitate phytoplankton growth. In particular, the increased residence time in the well-lit layer of the water column and the consequent increase in light exposure might have significant effects on the interactions between phytoplankton and grazers, potentially favouring the increase of phytoplankton biomass.

Previous laboratory and field studies have shown that under increasing light and temperature, the ratio of carbon to nutrient in phytoplankton increases (Urabe and Sterner, 1996; Hessen et al., 2002; Martiny et al., 2013) with significant consequences for the performance of grazers feeding on them (Urabe and Sterner, 1996; Hessen et al., 2002). Urabe and Sterner (1996), studying a predator-prey system comprising an alga prey consumed by a predatory zooplankton, found that (under experimental conditions) the growth of the grazer was related to the ratio between light and the limiting nutrient. Interestingly, the grazer growth rate was linearly related to the algal biomass only at low light intensity while, at increasing light levels, it started to decrease due to the decrease in the nutrient quality of the prey. This result was interpreted by invoking decoupling between photosynthesis and nutrient uptake which occurs under high light to nutrient ratio.

The cellular imbalance between carbon and nutrient made the algae less palatable for zooplankton. Unlike phytoplankton, zooplankton physiology does not allow a substantial variability of internal stoichiometry (Loladze et al., 2000, Siuda and Dam, 2010) and therefore requires nutrient rich prey to grow efficiently. Various studies have demonstrated that even small changes in phytoplankton stoichiometry can be associated with significant changes in food palatability and therefore affect zooplankton prey selection, physiological processes and thus efficiency (Flynn et al., 1996; Jones and Flynn, 2005). Loladze et al. (2000) proposed a model in which an increase in the carbon to nutrient ratio in

phytoplankton, triggered by an increase in light, induces a decrease in zooplankton (carbon) assimilation efficiency, concluding that an increase in energy (light) is not of advantage to the whole system but only for the primary producers (i.e. the paradox of energy enrichment).

Although these mechanisms are experimentally well documented and various theoretical and mechanistic models have been developed on them (Loladze et al., 2004; Hall et al., 2004; Mitra, 2006; Diehl, 2007; Stief et al., 2010; Elser et al., 2012), they have never been tested in relation to the phytoplankton bloom formation under realistic seasonally changing environmental conditions (i.e., nutrient and light). Furthermore, the effect of phytoplankton nutritional quality on grazers has never been implemented in a fully structured marine ecosystem model. Typically, marine ecosystem models are poor at describing zooplankton grazing as they often have very rigid food webs (Sailley et al., 2013; Mitra et al., 2014) and this strongly limits their utilization for the investigation of predator-prey dynamics.

The effect of phytoplankton quality (described as nutrient stoichiometry) on the ingestion and assimilation efficiencies of a consumer has been termed **S**toichiometric **M**odulation of **P**redation (SMP, Mitra 2006). The importance of inclusion of SMP when simulating planktonic predator-prey interactions against experimental datasets has been demonstrated for both micro- and meso-zooplankton (Mitra, 2006; Mitra and Flynn 2006; Mitra and Flynn 2007). Mitra (2006) in particular has shown that the inclusion of SMP in a zooplankton model significantly improved the simulation of the interactions between the microzooplankton *Oxyrrhis marina* and the phytoplankton *Isochrysis galbana* observed by Flynn and Davidson (1993). However, these studies have mainly focussed on model validation using laboratory data; i.e., SMP has not been tested in a realistic ecosystem framework.

104 In this paper, we have integrated the SMP (Mitra, 2006) into the European Regional Seas
105 Ecosystem Model (ERSEM, Blackford et al., 2004) with the aim to explore how the
106 combination of abiotic factors (e.g., NHF) and biotic mechanisms (e.g., SMP) impact on
107 plankton bloom dynamics. To this end, the revised version of ERSEM (hereafter ERSEM-
108 SMP) has been coupled with the General Ocean Turbulence Model (GOTM, Burchard et al
109 1999), implemented at the station L4 (50^{o} 15'N, 4^{o} 13'W) and tested against the high
110 frequency observations at that site. Our working hypothesis is that the increase in light
111 exposure experienced by diatoms in the transition between winter and spring may result in
112 changes in the internal stoichiometry of the diatoms, reducing grazing pressure and thence
113 favouring increase in their biomass.

114 We focus on station L4 because it has an extensive time series data of phytoplankton and
115 zooplankton abundance, coupled with measurements of physical properties and nutrients. In
116 addition to diatoms, the dominant primary producers, *Phaeocystis* blooms are also regularly
117 observed at this site with intense but short-lived peaks during spring. Coccolithophorids may
118 also occasionally bloom but rarely attain the high cellular density of diatoms (Widdicombe et
119 al., 2010). Microzooplankton are observed to peak concomitantly (typically ciliates) or just
120 after (heterotrophic dinoflagellates) the diatom bloom, albeit with high variability in timings
121 from year to year (Atkinson et al. this issue). This group achieves a higher biomass at L4 than
122 mesozooplankton (Atkinson et al. this issue) and due to higher specific metabolic rates is
123 likely to dominate the grazing impact (Calbet and Landry, 2004; Irigoien et al., 2005;
124 Bautista and Harris, 1992; Atkinson et al., unpublished data). Simulation of phytoplankton
125 internal stoichiometry and biomass, along with microzooplankton biomass, grazing and
126 assimilation efficiency were critically analysed and used to test our hypothesis. Simulated
127 diatoms, microzooplankton and nutrients were compared with available in situ data.

128

THE MODEL

ERSEM is a bulk biomass functional group ecosystem model describing the nutrient and carbon cycle within the lower trophic levels of the marine ecosystem. Model state variables include living organisms, dissolved nutrients, organic detritus, oxygen and CO_2. A key feature of ERSEM is the decoupling between carbon and nutrient dynamics allowing the simulation of variable stoichiometry within the modelled organisms. Chlorophyll is also treated as an independent state variable following the formulation proposed by Geider et al. (1996). Consequently, each plankton group is modelled using up to five state variables describing each cellular component: carbon, nitrogen, phosphorus, silicon (only for diatoms) and chlorophyll-a. These features make ERSEM particularly suitable for this work.

In order to test our hypothesis which specifically focuses on the diatoms-microzooplankton grazing interactions, we have simplified the standard ERSEM food web described in Blackford et al (2004) as shown in Fig. 1. The rationale behind this is to "isolate", as far as possible, the biotic processes to be investigated (e.g., diatom quality and allied impact on microzooplankton growth dynamics) and therefore making it easier to quantify their relevance. Thus, our model is based on a predator-prey system (accounting for SMP) comprising of diatoms (P1), considered as the dominant bloom-forming phytoplankton at L4 and microzooplankton (Z1) considered as the dominant grazers of diatoms; Z1 represents the fraction of microzooplankton (e.g., dinoflagellates such as *Gyrodinium* and *Protoperidinium*; ~ ESD > 20 µm) large enough to graze diatoms. To make the system more realistic and consistent with the L4 observations, we have also introduced a second phytoplankton functional group accounting for small (non-diatoms) phytoplankton (P2) and their grazers (Z2). P2 includes a variety of groups (e.g., nanoflagellates and *Phaeocystis*) expressing a wide range of traits and thus represents generic autotrophic activity at a lower size range; i.e.,

P2 has been included to ensure that diatoms have competitors for nutrients at the beginning of the bloom. Z2 represents the smaller fraction of microzooplankton (i.e., ciliates such as *Strombidium*) assumed to be specialised to feed on phytoplankton (mainly nanoflagellates) smaller than blooming diatoms.

Finally, a top closure mimicking the mesozooplankton grazing on microzooplankton is represented by Z3. The interactions between P2 and Z2, and Z3 and Z1 are modelled through the standard ERSEM formulation (Blackford et al., 2004) without the inclusion of SMP. Z2 and Z3 do not have predators within the model but they are assumed to cannibalize (Fig 1) and thus mimicking a density dependent top down closure. Bacteria are not explicitly modelled but are implicitly represented through remineralisation of detritus (equal to 0.05 d^{-1}) producing dissolved nutrients and CO_2.

As we focus on the formation and evolution of diatom blooms occurring between April and July we did not consider the autotrophic dinoflagellates, which usually bloom in late summer and/or early autumn (Widdicombe et al., 2010). It is worthwhile to recall that this simplified food web is not meant to represent the entire plankton community with allied complexities in their interactions as observed at L4, rather our aim is to focus on one specific process.

Silica regeneration in the water column is not considered in the standard ERSEM formulation where biogenic silica is assumed to be regenerated only via the benthic compartment. However, in order to prevent extreme silica limitation we have assumed a simple first order silica remineralisation converting biogenic particulate silica to dissolved silica at a fixed rate of 0.1 d^{-1}. This simple assumption is consistent with experimental evidences suggesting that up to 50% of the biogenic silica (opal) is re-generated in the euphotic zone (Sarmiento and Gruber, 2006).

A complete description of the equations, basic assumptions and underlying philosophy of ERSEM can be found in Blackford et al. (2004). Here we limit our description to the formulation describing Z1 which is the only part of the model altered with respect to the original model. The general equation for Z1 carbon biomass is given by the balance between grazing (gra), and loss terms due to respiration (res), excretion (exc), natural (non-predation) mortality ($mort$) and predation mortality ($pred$):

$$\frac{dZ}{dt} = \frac{dZ}{dt}\Big|^{gra} - \frac{dZ}{dt}\Big|^{res} - \frac{dZ}{dt}\Big|^{exc} - \frac{dZ}{dt}\Big|^{mort} - \frac{dZ}{dt}\Big|^{pred} \quad (1)$$

Grazing is described using a "potential" grazing term ($grazing'$) multiplied by a factor taking into account the nutritional quality of the prey:

$$\frac{dZ}{dt}\Big|^{gra} = grazing' * FQ \quad (2)$$

FQ is the function linking the potential grazing to the stoichiometry of phytoplankton described below (equation 6). $grazing'$ is described using the classical Michaelis-Menten formulation as reported in Blackford et al., (2004):

$$grazing' = Z * temp * r\frac{P\prime}{P\prime + K} \quad (3)$$

Where Z is the zooplankton biomass, $temp$ is a function accounting for the temperature dependency, r the potential grazing rate and P' the available food. K is the half saturation constant for food. P' is given by the biomass of the prey (P) multiplied by a parameter representing the "preference" for that particular prey (P_f) and scaled by a Michaelis Menten

function accounting for a food threshold parameter ($minfood$) which prevents excessive grazing of scarce prey:

$$P' = P_f * P * \frac{P}{P+minfood} \quad (4)$$

The function $temp$ describes an enhancement of physiological processes with the increase of temperature following a Q_{10} function:

$$temp = Q_{10}^{\left(\frac{(T-10)}{10}\right)} \quad (5)$$

FQ is a function linking the grazing with the nutritional quality of the phytoplankton, described here using nutrient stoichiometry and is given by:

$$FQ = 1 + \left[1 - min\left(\frac{qpP}{qpZ}, \frac{qnP}{qnZ}, 1\right)\right] * a \quad (6)$$

where qpP and qpZ are the phosphorus to carbon (P:C) ratios of phytoplankton and zooplankton respectively, and qnP and qnZ are the nitrogen to carbon (N:C) ratios in phytoplankton and zooplankton respectively. a is the parameter describing the response of the grazers to the decrease in quality of the prey (Mitra, 2006). In this work we have assumed a decrease of ingestion associated with low nutrient content of the prey (i.e., decrease in palatability) and as such, we have considered a equal to -1.

Respiration is composed of a basal component (depending on biomass) and a metabolic-activity related component (depending on ingestion):

$$\left.\frac{dZ}{dt}\right|^{res} = R_r * temp * Z + \left.\frac{dZ}{dt}\right|^{gra} * A_r * AE \quad (7)$$

Assimilation efficiency (AE) is assumed to vary between a minimum and a maximum value (assumed to be 0.25 and 0.75, respectively) and is given by:

$$AE = AE_{min} + (AE_{max} - AE_{min}) * FQ_{AE} \quad (8)$$

where FQ_{AE} is the function linking the phytoplankton quality (C:N:P) to the assimilation efficiency of zooplankton (Mitra, 2006) and is given by:

$$FQ_{AE} = \min(1, N_{lim}, P_{lim}) * (1 + K_{AE}) min\left(1, \frac{qpP}{qpZ}, \frac{qnP}{qnZ}\right) \quad (9)$$

In Eq. 9, K_{AE} is the half saturation constant as described in Mitra (2006)

N_{lim} and P_{lim} are two Michaelis Menten-like functions given by:

$$N_{lim} = \frac{\frac{qnP}{qn_{max}}}{\frac{qnP}{qn_{max}} + K_{AE}} \quad (9.1)$$

and

$$P_{lim} = \frac{\frac{qpP}{qp_{max}}}{\frac{qpP}{qp_{max}} + K_{AE}} \quad (9.2)$$

qp_{max} and qn_{max} are the maximum phytoplankton P and N quota (i.e., N:C and P:C ratios), respectively, assumed to be equal to the double of the nutrient content implied by the Redfield ratio (Blackford et al., 2004, Table 3)

Loss term due to excretion is governed by the following equation:

$$\left.\frac{dZ}{dt}\right|^{exc} = \left.\frac{dZ}{dt}\right|^{gra} * (1 - AE) \quad (10)$$

Non-predation mortality loss is assumed to be composed by a constant term plus an additional fraction triggered by low oxygen concentration

$$\left.\frac{dZ}{dt}\right|^{mort} = Z * \left((1 - eO_2) * r_{mortox} + r_{mort}\right) \quad (11)$$

235 r_{mort} and r_{mortox} are the background mortality rate and the mortality rate at low oxygen
236 concentration, respectively. eO_2 is an oxygen limitation factor calculated from the relative
237 oxygen saturation (O_{rel}) and the half saturation mortality rate constant (h_{oxmort}):

238 $$eO_2 = (1 + h_{oxmort}) * \left(\frac{O_{rel}}{O_{rel}+h_{oxmort}}\right) \quad (12)$$

239 The ingestion of nutrient via grazing is derived by equation 3 and reflects the nutrient content
240 of the ingested prey. In the same way, the loss of nutrient via excretion, mortality and
241 predation is depending on the carbon to nutrient ratio of zooplankton. Additionally, any
242 nutrient in excess of a threshold value ($qZ_{max}^{N.P}$) is assumed to be directly excreted to the
243 inorganic pool (phosphate and ammonium).

244 Model parameters describing the communities Z1, Z2 and Z3 are listed in Table 1. The
245 parameters for the phytoplankton functional groups P1 and P2 are the same as in Blackford et
246 al., (2004). However, a few changes were required to improve our simulation at L4: i) the
247 potential photosynthetic rate of P2 was lowered from 2.7 to 2.0 d^{-1}; ii) different maximum
248 chlorophyll to carbon ratios were employed for the two phytoplankton groups (0.04 for P1
249 and 0.03 for P2; consistent with literature values (Geider et al. 1997)), and iii) the reference
250 silica to carbon ratio for diatoms has been lowered to 0.01 (mmol S (mg C)$^{-1}$) as reported in
251 Vichi et al. (2006).

252

253

254

255

256

PHYSICAL SETUP AND OBSERVATIONAL DATA

The GOTM-ERSEM set up used in this work is identical to that described in Polimene et al., (2014). The model is forced with reanalysis meteorological data (ECMWF) and initialised with temperature, salinity and nutrient concentrations observed *in situ* (Smyth et al., 2010). At the lower boundary of the water column a simple remineralisation closure is applied exporting sinking detritus that is re-injected into the water column as dissolved nutrients and inorganic carbon at a fixed rate of 0.05 d^{-1}.

Surface radiation is calculated by an astronomical formula (Rosati and Miyacoda, 1988) taking into account latitude, longitude, time, fractional cloud cover and albedo. Light extinction through the water column is assumed to be dependent on water mass, i.e. organic particulates in the water column (both living and detritus) and silt, as described in Blackford et al (2004). The total surface heat flux Q_{tot} is calculated as the sum of the latent heat flux Q_E, the sensible heat flux Q_H, and the long wave back radiation Q_b. Each of these fluxes are calculated by using the bulk formulae of Kondo (1975). The net heat flux (NHF) is then calculated by summing the incident short wave radiation to the total heat fluxes. The model was run for 10 years (2000-2009) after 4 years of spin up.

The observational data used in this work (Woodward et al., 2013; Widdicombe et al 2010) were obtained under the weekly sampling strategy of the Western Channel Observatory (WCO, http://www.westernchannelobservatory.org.uk/). The description of the methodology used for samples collection and cell enumeration of phytoplankton and microzooplankton can be found in Widdicombe et al., (2010). Cell volumes are calculated according to the equations of Kovala and Larrance (1996) and converted to carbon using the equations of Menden-Deuer and Lessard (2000).

281 SENSITIVITY ANALYSIS

282 A quantitative sensitivity analysis (SA) was carried out to investigate the changes introduced
283 by the SMP formulation to the ERSEM simulations. We applied a Monte-Carlo based
284 approach (see, e.g., Saltelli et al, 2005, Pastres and Ciavatta, 2005) to rank the sensitivities of
285 a target model output y (the annual average of the grazing efficiency) with respect to the
286 model parameters that were handled in this work (i.e., the parameters in Table 1 and the
287 phytoplankton parameters altered with respect to Blackford et al., (2004)). The SA included
288 also the initial conditions of nitrate and phosphate. The *m* model parameters and nutrient
289 initial conditions defined the "input factor" vector (Table 2) of the SA, $\mathbf{X_i} = (X_1,.., X_j,$
290 $\ldots,X_m)$. A number (i=1,2,…,) of n random realizations of the vector were obtained by
291 sampling uniform probability distributions defined for the input factors (Table 2). Each
292 realization is used to run a model simulation that provides a scalar output y_i.

293 The input-output relationship was represented by means of a multiple linear regression model
294 $\mathbf{y = X\ b + \varepsilon}$, and the *m* absolute values of the standardized regression coefficients β_j are the
295 sensitivity indices that provides the rank of the input factors (e.g. Saltelli et al., 2000; Pastres
296 and Ciavatta, 2005). The SA was carried out, for both ERSEM and ERSEM SMP, by running
297 n=1000 model simulations of the year 2000, after a four year spin-up. The same probability
298 density functions of the input factors were applied in the two model configurations to make
299 the rankings inter-comparable. The rankings of the parameters for the two models (ERSEM
300 and ERSEM-SMP) were compared to discuss the importance of the SMP "mechanism" with
301 respect to the tuning of the model parameters in simulating the target variable.

302 We note that the regression coefficients provide meaningful rankings only when the linear
303 model explains relatively large fractions of the model output variability (Saltelli et al., 2000).
304 In our application we verified that the determination coefficients (R^2) of the linear models

were higher than 70% and statistically significant (F-statistic for linear versus constant model; $p<0.001$).

RESULTS

Simulated and observed, monthly averaged, diatoms and microzooplankton biomass, nitrate phosphate and silicate are displayed in Fig 2. The qualitative agreement between model and observations is evaluated through the Spearman's correlation index between simulated and observed variables shown in Table 3. The correlation coefficient is higher than 0.6 for microzooplankton and nutrients and equal to 0.35 for diatoms. The correlation indices concerning the simulations carried out with the standard ERSEM model are also reported for comparison.

The seasonal evolution of simulated air-sea net heat flux (NHF), surface turbulent kinetic energy (TKE) and mixed layer depth (MLD) is depicted in Fig 3. NHF is negative from January to March, switching to positive in April. After the summer, NHF reverts back to negative in September. The transition between winter and spring (March-April) is also characterized by a reduction in TKE (from 0.0007 to < 0.0004 m^{-2} s^{-2}).TKE increases after the summer, returning to values comparable with those simulated in winter. The simulated seasonal cycle of the MLD implies that in April and May phytoplankton are exposed more to light due to being "confined" in the first 10-15 metres of the water column. Simulated average irradiance within the mixed layer depth is 24 W m^{-2} in March and 115 W m^{-2} in April. These results are consistent with the description of the physical conditions underpinning the onset of phytoplankton bloom reported in Smyth et al. (2014).

Figure 4 shows that the diatom carbon to phosphorus and carbon to nitrogen ratios are low in winter, they start to increase in spring (corresponding with the bloom) reaching the maximum level in summer. It is worth noting that the carbon to nutrient ratios simulated in all our experiments are comparable with the values reported in literature for marine particulate organic matter (Geider and La Roche, 2002). Microzooplankton assimilation efficiency follows the opposite trend being high in winter, decreasing in spring (in correspondence of the sharp increase of diatoms biomass) and reaching the lowest level in summer. The grazing flux, in contrast, reaches the maximum level in May, corresponding to the highest diatom biomass.

Higher phytoplankton biomass (Fig. 5) does not correspond to higher nutrient content which, in contrast, coincides with the higher zooplankton assimilation efficiency. Notably, the grazing flux, when taken on a daily basis, is less tightly related to the prey biomass. Higher grazing rates, correspond to intermediate levels of biomass (between 50 and 150 mg C m^{-3}) and an intermediate level of the prey nutrient quota (C:P ~80-95 and C:N ~4-5.5). Diatoms, at the peak of the bloom (Fig. 6), are characterized by a decrease in the nutrient to carbon ratios with respect to pre bloom conditions. The declining part of the bloom is characterized by a slow increase in cellular nutrient content due to the release of carbon via exudation (Fig. 6) which enhances grazing activity. As a result, the grazing flux and the microzooplankton biomass reach the highest value at the end of the bloom.

The sensitivity of the ERSEM-SMP model to decrease in the concentrations of phosphate and nitrate, given as model initial conditions (50% reduction was investigated) is shown in Fig. 7 and Fig. 8. Lowering nutrient concentrations causes diatoms to become more nutritionally imbalanced and therefore, less palatable to zooplankton. This leads to a counterintuitive response that fewer nutrients produce a higher peak (in term of carbon) during the bloom (Fig. 7). A simulation carried out by decreasing nitrate and phosphate initial conditions by

352 25% (data not shown) showed the same qualitative (but less intense) response, with a slight
353 increase in diatom carbon biomass and a concomitant decrease in zooplankton biomass. Only
354 when the initial nitrate and phosphate conditions are decreased by 75% (data not shown) do
355 we see a clear decrease in diatom biomass. Model simulations performed with the standard
356 ERSEM formulation (i.e. without SMP, and a fixed assimilation efficiency of 50%) applied
357 to the same model foodweb (Fig 1) are shown in Fig 9. In this case diatoms never manage to
358 bloom and the system is dominated by microzooplankton. By decreasing the initial
359 concentration of nitrate and phosphate by 50%, the system does not show substantial changes
360 in behaviour (Fig. 10).

361 A Monte Carlo based sensitivity analysis on both ERSEM-SMP and ERSEM has been
362 performed in order to assess to what extent the above described results are affected by the
363 choice of selected parameters and nutrient initial conditions (Table 2). As the essence of the
364 SMP is the effect of the phytoplankton nutritional status on the grazing activity, we have
365 selected as target variable of our analysis the grazing efficiency of the model
366 microzooplankton Z1. The results of this analysis are presented in Table 4 where each input
367 factor (Table 2) is ranked on the base of its capacity to affect the simulation of the target
368 variable. In both the models, the parameters defining the half saturation constant for food and
369 prey "preference" (K(Z1) and Pf(P1-Z1), respectively) are the most important. However,
370 Table 4 highlights that with the addition of the SMP, the initial condition of the limiting
371 nutrient is considerably more important for the simulation of the grazing activity of Z1 over
372 P1. PO_4 in table 4 ranked 6^{th} and 18^{th} for ERSEM-SMP and ERSEM, respectively.
373 Furthermore, the ERSEM-SMP simulations of grazing efficiency have relatively low
374 sensitivity with respect to the values of the SMP-parameters. Indeed, the new parameters
375 introduced for the implementation of the SMP (AE_{max}, AE_{min}, and K_{AE}) ranked relatively low
376 (9, 17 and 24, respectively). This suggests that the ERSEM-SMP simulations depend more on

the process/mechanism described in the model than on the numerical values of the parameters.

An additional sensitivity analysis has been performed by manually altering some key zooplankton parameters and nutrient initial condition (Table 5) in the ERSEM model (Fig. 11). The rationale behind this experiment was to further investigate whether, by tuning specific parameters, the standard ERSEM can produce simulations comparable to the ones of ERSEM-SMP.

Figure 11 shows that by changing the half saturation constant for food (K) and the food threshold ($minfood$), the simulation does not display significant changes: the system is, in all the three experiments, dominated by microzooplankton. Only by assuming a greater predatory pressure on microzooplankton (by increasing the value of the parameter P_f, experiment S5) do diatoms manage to bloom exceeding zooplankton biomass. The sensitivity experiment S5 is the model setup under which ERSEM produces the closest simulation to ERSEM-SMP. However, even under these conditions, by reducing the initial nutrient conditions by 50% the standard ERSEM does not display the behaviour simulated by the SMP-ERSEM model, further confirming the results displayed in Table 4.

DISCUSSION

Our simulations suggest that the increase in light exposure experienced by diatoms between March and April decouples photosynthesis from nutrient uptake, thereby altering cellular stoichiometry. The increase in the cellular carbon to nutrient ratio of the diatoms decreases their palatability thence reducing both grazing and assimilation efficiency of the microzooplankton. We suggest that these changes contribute to the formation of the diatom

400 bloom regularly observed at the station L4. A conceptual model describing the formation and
401 evolution of a diatom bloom is depicted in Fig. 12.

402 During winter, diatoms are limited by the amount of light but are also controlled through
403 grazing pressure exerted by large microzooplankton (modelled through the variable Z1).
404 During this time of the year, high environmental nutrient concentrations allow diatoms to be
405 rich in nutrients (such as N and P) and, consequently, zooplankton assimilation efficiency is
406 also high. Changes in physical conditions, such as reduced turbulence and increased surface
407 water temperature (Smyth et al., 2014 and Fig 3), increases the phytoplankton residence time
408 in the well-lit zone of the water column (Fig 3) and desynchronize photosynthesis from
409 nutrient uptake. This increases the amount of cellular carbon with respect to nutrients. Less
410 nutrient content, decreasing diatom palatability, reduces the activity of microzooplankton,
411 allowing diatoms to "escape" from being top down controlled and thus to bloom.

412 Bloom conditions for diatoms are therefore a compromise between attaining high nutrient
413 cellular content (i.e., high food quality), where the diatom population are controlled by
414 zooplankton grazing, and poor nutrient cellular content under which diatoms (although
415 "escaping" zooplankton grazing) are too nutrient stressed for growth. The former condition
416 takes place in winter, the latter in summer. The conditions leading to the bloom occur in the
417 spring period when the nutrient condition of diatoms are at an intermediate level which still
418 allows a positive growth but, at the same time, a reduced palatability.

419 The idea that reduced cell nutrient content be advantageous for primary producers has been
420 previously used in evolutionary modelling work (Branco et al., 2010). The generic model
421 proposed by these authors implied that phytoplankton with intermediate nutrient uptake rates
422 are less palatable for herbivores. In this way, some phytoplankton species gain a competitive
423 advantage over competitors that have higher affinity for nutrients and are therefore more

susceptible to grazers. Here, we have shown that the same concept can be important within a single phytoplankton group on a seasonal scale.

Including SMP makes the modelled predator-prey interactions sensitive to the availability of nitrate and phosphate. As expected, the simulations with low nutrient concentrations show that diatoms are more stoichiometrically imbalanced and therefore less palatable for zooplankton when the availability of nitrate and phosphate is low. Consequently, diatoms produce a higher peak (in terms of carbon) during the bloom (Fig. 5). This suggests that decreasing the food quality (more than the quantity) of primary producers, reduces the transfer of carbon from the algal producers to the higher trophic levels of the food chain. This may have profound effects on the ecosystem responses to climate change, particularly in regions where the surface waters are expected to become more oligotrophic (Polovina et al., 2008). Sensitivity experiments showed in Table 4 and Fig. 11 show that the standard ERSEM grazing parameterisation does not reproduce this kind of dynamics. More in general, the sensitivity analysis highlights that the SMP as "mechanism" is more relevant in impacting the model simulation of the grazing efficiency then the numerical values of the parameters used. This strengthens the case for exploring the inclusion of SMP in marine ecosystem models used for climate change simulations.

Particular attention should be paid to the role of silica in the aforementioned mechanism. Silica is not required for zooplankton growth and therefore is not included in the SMP formulation implemented here. Furthermore, silica is assumed to limit directly primary production in ERSEM (Ebenhoh et al., 1997; Blackford et al., 2004) with the consequence that silica is coupled more with carbon than nitrogen or phosphorous. Reduced availability of silica also implies a reduced fixation of carbon and therefore a more balanced carbon to nitrogen and phosphorus cellular ratio. Consequently, the above described dynamics is not simulated when silica is the limiting nutrient.

449 The importance of food quality as a consequence of skewed nutrient stoichiometry which in
450 turn is induced by an "imbalance" in the supply of nutrients and light has previously been
451 stressed in laboratory experiments (Urabe and Sterner, 1996; Hessen et al., 2002) and
452 theoretical modelling studies (Loladze et al., 2000; Loladze et al., 2004; Hall et al., 2004;
453 Mitra, 2006; Diehl, 2007; Elser et al., 2012). We have related phytoplankton palatability to
454 the physical environment (Fig. 3) and have proposed a conceptual model (Fig. 12), describing
455 bloom formation and evolution, which connects physical constrains (heat flux, turbulence,
456 mixed layer depth) physiological status of phytoplankton (i.e., cellular stoichiometry) and
457 grazing. These connections are summarised in Fig. 13 which shows the correlation between
458 heat fluxes and cellular stoichiometry($r=0.88$, $p<0.001$), an emergent property of our model.
459 While confirming that the switch of NHF from negative to positive described by Smyth et al.
460 (2014) is a prerequisite for the bloom formation, our model also suggests that, after the onset
461 of the proper physical conditions, phytoplankton decrease in palatability and reduced
462 zooplankton grazing pressure play a significant role in the formation of a bloom.

463 We have shown that a combination of abiotic and biotic factors work synergistically to
464 impact on the plankton bloom dynamics. The behaviour shown by the present model is
465 consistent with the "paradox of energy enrichment" hypothesised by Loladze et al. (2000):
466 when more energy is supplied to the system (steep increase in light) a decoupling between
467 carbon and nutrient is induced. The latter decreases the "quality" of the prey which, being
468 less suitable for the predator, reaches its highest concentration. Our model also supports the
469 general concept of the "loophole" hypothesis (Irigoien et al., 2005; Kiørboe, 2008). These
470 authors, investigating the biological dynamics underpinning a phytoplankton bloom invoked
471 a set of mechanisms including physical (e.g., size, colony-formation, spines, frustules and
472 coccoliths) and chemical (e.g., DMSP production) defence leading to a decrease of
473 palatability of phytoplankton and to a decrease (loophole) of the grazing pressure. Our

474 simulations and the consequent conceptual model depicted in Fig.12 suggest that the decrease
475 of the phytoplankton nutrient to carbon ratio (and the subsequent decrease in phytoplankton
476 palatability) could play a pivotal role in creating the "loophole" through which diatoms
477 manage to bloom.

478 Although these results support our hypothesis, we recognise that only with specific,
479 purposely performed, field measurements will we be able to properly assess the mechanism
480 described in Fig. 12. In particular, we require data on the temporal evolution of the
481 phytoplankton cellular nitrogen and phosphorus with respect to carbon content; these are
482 currently lacking. Also, time series measurements of micro- and meso-zooplankton grazing,
483 looking both at mass specific ingestion rates and total grazing pressure, would shed light on
484 the complex dynamics surrounding the start of a bloom. One of the advantages of modelling
485 work like this is to highlight gaps and inconsistencies in current knowledge and datasets, and
486 thence to inform and drive future experimental research.

487

488 **ACKNOWLEDGMENTS**

489 The authors would like to thank the PML crew of RV Quest and the PML staff involved in
490 the sampling of the Plymouth L4 site. Nutrient data used in Fig 2 were analysed by Carolyn
491 Harris and Malcolm Woodward.

492 LP was part funded by the EC FP7 My Ocean project. AA and LP were part funded through
493 the UK NERC-Defra Shelf Seas Biogeochemistry program. JIA and AM were part funded
494 thought the EC FP7 Euro Basin project. AM was part funded by the NERC UK project

495 iMarNet NE/K001345/1. SC was part funded by the NERC National Centre of Earth
496 Observation (NCEO). AA, CW, JIA, LP, SS and SC were part funded through NERC
497 National Capability, in sustained observations and marine modelling.

498

499 **Table 1.** Zooplankton parameters

Prameter	Notation	Unit	Z1	Z2	Z3	Reference
Q_{10} value	Q_{10}	adim	2	2	2	Blackford et al (2004)
Grazing rate at 10 C	r	d^{-1}	1.2	2.0	0.5	Blackford et al (2004)
Half saturation constant for food	K	mg C m^{-3}	10	10	40	This study/ Blackford et al (2004)
Food threshold	$minfood$	mg C m^{-3}	2.5	10	1.0	This study/ Blackford et al (2004)
Fraction of food respired	A_r	d^{-1}	0.5	0.4	0.6	This study/ Blackford et al (2004)
Constant Assimilation efficiency (Z2 and Z3)	AE	adim	N/A	0.5	0.5	Blackford et al (2004)
Min Assimilation efficiency	AE_{min}	adim	0.25	N/A	N/A	This study
Max Assimilation efficiency	AE_{max}	adim	0.75	N/A	N/A	This study
Half saturation constant for AE	K_{AE}	adim	1			Mitra (2006)
Rest respiration rate	R_r	d^{-1}	0.02	0.02	0.02	Blackford et al (2004)
Mortality rate	r_{mort}	d^{-1}	0.05	0.05	0.05	Blackford et al (2004)
Mortality rate due to low oxygen	r_{mortox}	d^{-1}	0.25	0.25	0.25	Blackford et al (2004)
Michaelis Menten constant for oxygen limitation	h_{oxmort}	mmol m^{-3}	7.8125	7.8125	7.8125	Blackford et al (2004)
Max N:C	qZ_{max}^{N}	mmol N $(mg C)^{-1}$	0.0167	0.0167	N/A*	Blackford et al (2004)
Max P:C	qZ_{max}^{P}	mmol P $(mg C)^{-1}$	0.001	0.001	N/A*	Blackford et al (2004)
Available fraction of prey (P1 for Z1, P2 for Z2 and Z1 for Z3)	P_f	adim	1	1	0.5	This study

500 *Mesozooplankton are assumed to have a fixed internal stoichiometry (Blackford et al.,
501 2004)

502

503

504

505

506

507

508

509

Table 2 Input factors of the Monte Carlo based sensitivity analysis, their nominal values and the range minimum-maximum of their uniform probability distributions. The notations of the parameters are specified in Table 1 (but see notes c and d)

Notation	Nominal	minimum	Maximum	Notes
K(Z1)	10	1	60	
Pf(P1-Z1)	1	0.1	1	
Chl:Cmax(P1)	0.04	0.01	0.07	c
K(Z3)	40	1	60	
Pf(P2-Z2)	1	0.1	1	
PO_4	0.4	0.2	0.6	d
r(Z1)	0.02	0.014	0.026	*
K(Z2)	10	1	60	
AEmax(Z1)	0.25	0.1	0.499	a
qZPmax(Z1)	0.0167	0.01169	0.02171	*
Ar(Z1)	0.5	0.35	0.65	*
rmort(Z1)	0.25	0.175	0.325	*
minfood(Z1)	2.5	1	20	
Pf(Z1-Z3)	0.5	0.1	1	
qsP1c	0.01	0.01	0.03	c
NO_3	8	4	12	d
AEmin(Z1)	2	1.4	2.6	*a
r(Z2)	1.2	0.84	1.56	*
Q10(Z1)	0.4	0.28	0.52	*
Rr(Z1)	0.05	0.035	0.065	*
Ar(Z2)	0.5	0.35	0.65	*
Q10(Z2)	2	1.4	2.6	*
r(Z3)	0.5	0.35	0.65	*
KAE(Z1)	0.75	0.5	0.9	a
minfood(Z3)	1	0.1	10	
qZPmax(Z2)	0.0012	0.00084	0.00156	*
qZNmax(Z1)	2	1.4	2.6	*
Chl:Cmax(P2)	0.03	0.01	0.07	c
r(P2)	2	1.5	3	c
rmortox(Z3)	0.25	0.175	0.325	*
rmort(Z3)	0.05	0.035	0.065	*
AE(Z3)	0.5	0.1	0.9	
hoxmort(Z3)	7.8125	5.46875	10.15625	*
hoxmort(Z1)	7.8125	5.46875	10.15625	*
Rr(Z2)	0.02	0.014	0.026	*
Rr(Z3)	0.02	0.014	0.026	*
minfood(Z2)	10	1	20	
rmort(Z2)	0.25	0.175	0.325	*
AE(Z2)	0.5	0.1	0.9	
rmortox(Z1)	0.001	0.0007	0.0013	*
qZNmax(Z2)	0.0167	0.01169	0.02171	*
Q_{10}(Z3)	2	1.4	2.6	*
hoxmort(Z2)	7.8125	5.46875	10.15625	*
rmortox(Z2)	0.05	0.035	0.065	*
AE(Z5)	0.5	0.1	0.9	b

Notes. * : the range minimum-maximum is defined as the nominal value ±30% of the value itself; a) parameters included in ERSEM SMP only; b) parameters included in ERSEM only; c) phytoplankton parameters for P1 and P2 not defined in Table 1 (Chl:Cmax = maximum chlorophyll-to-carbon ratio [mgChl $(mgC)^{-1}$]; r = potential photosynthetic rate [d^{-1}]; qsP1c = maximum silica to carbon ratio in diatoms [mmolSi $(mgC)^{-1}$]); d) initial conditions of nutrients (PO4 = phosphate [mmol m^{-3}]; NO3 = nitrate [mmol m^{-3}]).

Table 3. Spearman rank correlation between modelled and observed variables ($p<0.001$)

	diatoms	**microzoo**	**PO_4**	**NO_3**	**Si**
ERSEM-SMP	0.35	0.80	0.61	0.80	0.67
ERSEM	-0.16*	0.82	0.65	0.81	0.65

*p=0.07

Table 4. Results of the Monte Carlo sensitivity analysis of ERSEM SMP (left) and ERSEM (right). Ranking of the input factors (i.e. model parameters and initial conditions of nitrate and phosphate) based on computed standardized linear regression coefficients β. N.S. indicates parameters having β values that were not significantly different from zero (t-statistic; $p < 0.05$).

ERSEM SMP	Rank	ERSEM	Rank
K(Z1)	1	K(Z1)	1
Pf(P1-Z1)	2	Pf(P1-Z1)	2
Chl:Cmax(P1)	3	K(Z3)	3
K(Z3)	4	Pf(P2-Z2)	4
Pf(P2-Z2)	5	K(Z2)	5
PO_4	6	Chl:Cmax(P1)	6
r(Z1)	7	minfood(Z1)	7
K(Z2)	8	Pf(Z1-Z3)	8
AEmax(Z1)	9	r(Z1)	9
qZPmax(Z1)	10	qsP1c	10
Ar(Z1)	11	Ar(Z1)	11
rmort(Z1)	12	r(Z3)	12
minfood(Z1)	13	minfood(Z2)	13
Pf(Z1-Z3)	14	r(Z2)	14
qsP1c	15	r(P2)	15
NO_3	16	Ar(Z2)	16
AEmin(Z1)	17	minfood(Z3)	17
r(Z2)	18	PO_4	18
Q10(Z1)	19	NO_3	19
Rr(Z1)	20	AE(Z3)	20
Ar(Z2)	21	rmort(Z1)	21
Q10(Z2)	22	Chl:Cmax(P2)	22
r(Z3)	23	Q10(Z1)	23
KAE(Z1)	24	rmort(Z3)	24
minfood(Z3)	25	Rr(Z1)	25
qZPmax(Z2)	26	Q10(Z2)	26
qZNmax(Z1)	27	rmortox(Z3)	N.S
Chl:Cmax(P2)	28	Rr(Z2)	N.S
r(P2)	29	Q_{10}(Z3)	N.S
rmortox(Z3)	N.S	qZPmax(Z1)	N.S
rmort(Z3)	N.S	hoxmort(Z3)	N.S
AE(Z3)	N.S	rmort(Z2)	N.S
hoxmort(Z3)	N.S	hoxmort(Z1)	N.S
hoxmort(Z1)	N.S	AE(Z2)	N.S
Rr(Z2)	N.S	Rr(Z3)	N.S
Rr(Z3)	N.S	qZPmax(Z2)	N.S
minfood(Z2)	N.S	qZNmax(Z2)	N.S
rmort(Z2)	N.S	rmortox(Z2)	N.S
AE(Z2)	N.S	qZNmax(Z1)	N.S
rmortox(Z1)	N.S	hoxmort(Z2)	N.S
qZNmax(Z2)	N.S	AE(Z1)	N.S
Q_{10}(Z3)	N.S	rmortox(Z1)	N.S
hoxmort(Z2)	N.S		
rmortox(Z2)	N.S		

540

Table 5. Sensitivity experiments on key zooplankton parameters for the standard ERSEM model

experiment	**Parameters**		
	K	$minfood$	P_f (Z1 for Z3)
S1	45	2.5	0.5
S2	60	2.5	0.5
S3	60	10	0.5
S4	60	10	0.8
S5	60	10	1.0
S6	As S5 but with reduced (50%) initial nutrient (N and P) conditions		

569 **FIGURE CAPTIONS**

570 **Fig 1**. Schematic of the modelled food interactions. Dotted arrows indicate density-dependent
571 mortality closure, for example cannibalism

572 **Fig 2**. Modelled and observed time series of (A) diatom biomass; (B) microzooplankton
573 biomass; (C) phosphate; (D) nitrate; (E) silicate. Both observations and simulations are
574 monthly averages for the period 2000-2009. Units are mg C m^{-3} for biomasses and mmol m^{-3}
575 for nutrients. Modelled microzooplankton is the sum of Z1 and Z2.

576 **Fig 3.** Climatological, monthly averaged, simulated (A) Net Heat Flux (NHF, W m^{-2}); (B)
577 surface Turbulent Kinetic Energy (TKE, m^{-2} s^{-2}) and (C) Mixed Layer Depth (MLD, metres)

578 **Fig 4.** Climatological, monthly averaged, simulated diatom (P1) and microzooplankton (Z1)
579 (mg C m^{-3}) seasonal cycles. Colours refer to (A) diatom molar C:P; (B) diatom molar C:N
580 ratios; (C) microzooplankton (Z1) assimilation efficiency (Zeff) and (D) grazing (Z1 over P1,
581 mg C m^{-3} d^{-1}).

582 **Fig 5**. Scatter plots of modelled diatom (P1) biomass (mg C m^{-3}) and carbon to nutrient molar
583 ratios. Colour scales indicate: (A) and (B) microzooplankton (Z1) assimilation efficiency
584 (Zeff); (C) and (D) grazing (Z1 over P1, mg C m^{-3} d^{-1}). Simulations refer to daily averaged
585 surface values for the period 2000-2009

586 **Fig. 6.** (A) simulated Z1-P1 predator-prey system (biomasses and grazing) and (B) specific
587 carbon exudation rate subsampled from the modelled time series. Biomass is given in mg C
588 m^{-3}, grazing in mg C m^{-3} d^{-1} and the carbon specific exudation rate in d^{-1}. Colours refer to
589 diatom molar C:P.

590 **Fig. 7.** Simulated diatom (P1) and microzooplankton (Z1) seasonal cycle as in Fig. 4, but
591 with reduced (by 50%) nitrate and phosphate as initial conditions.

592 **Fig. 8**. Scatter plots as in Fig. 5 but with reduced nitrate and phosphate concentration as
593 initial condition. Nutrient concentrations were reduced by 50%.

594 **Fig. 9**. Climatological (2000-2009) diatom (P1) and microzooplankton (Z1) monthly
595 averaged seasonal cycles simulated with the standard ERSEM formulation. Colours refer to:
596 (A) C:P diatom molar ratio; (B) C:N diatom molar ratios and (C) grazing (Z1 over P1, mg C
597 m^{-3} d^{-1}).

598 **Fig. 10.** Simulated diatom (P1) and micrzooplankton (Z1) seasonal cycle as in Fig 8 but with
599 reduced (by 50%) nitrate and phosphate initial conditions.

600 **Fig. 11.** Monthly averaged, diatoms (P1) and microzooplankton (Z1) biomass (mg C m^{-3})
601 simulated in the sensitivity experiments described in Table 3.

602 **Fig. 12.** Conceptual model describing the formation and evolution of a diatom bloom. Biotic
603 processes are highlighted in blue. Red arrows imply the action of physical forcing such as
604 NHF, TKE and MLD.

605 **Fig. 13.** Scatter plot ($r=0.8$, $p<0.001$) between simulated diatom (P1) carbon to phosphorus
606 ratio (mol mol^{-1}) and NHF (W m^{-2}). Colorbar refers to microzooplankton (Z1) assimilation
607 efficiency (Zeff).

608 REFERENCES

609

610 Atkinson, A., Harmer, R.A., Widdicombe, C.E. McEvoy, A.J., Smyth, T.J., Cummings, D.G.,
611 Somerfield, P.J., Maud, J.L. McConville, K. (in review) Questioning the role of phenology
612 shifts and trophic mismatching in a planktonic food web.

613

614 Baretta, J.W., Ebenhoh, W. and Ruardij, P., 1995. The European regional Seas Ecosystem
615 Model, a complex marine ecosystem model. Neth. J. Sea Res., 33, 233–246

616

617 Bautista, B., Harris, R.P., 1992. Copepod gut contents, ingestion rates and grazing impact on
618 phytoplankton in relation to size structure of zooplankton and phytoplankton during a spring
619 bloom. Mar. Ecol. Prog. Ser. 82, 41-50.

620

621 Blackford, J. C., Allen, J. I., Gilbert, F. J., 2004. Ecosystem dynamics at six contrasting sites:
622 a generic modelling study. J. Mar. Syst., **52**,191-215.

623

624 Branco, P., Stomp, M., Egas, M., Huisman J., 2010. Evolution of nutrient uptake reveals a
625 trade-off in the ecological stoichiometry of plant herbivore interactions. Am. Nat., 176, 162-
626 176

627

628 Burchard, H., Bolding, K., Villareal, M. 1999 GOTM: a general ocean turbulence model.
629 Theory, applications and test cases. Technical Report EUR 18745 EN, European Commission

630

631 Calbet, A., Landry, M. R., 2004. Phytoplankton growth, microzooplankton grazing, and
632 carbon cycling in marine systems. Limnology and Oceanography; 49:51-57.

633

634 Diehl, S., 2007. Paradoxes of enrichment: Effects of increased light versus nutrient supply on
635 pelagic producer–grazer systems. American Naturalist 169, E173–E191.
636

637 Ebenhoh, W., Baretta, J.W., Baretta-Bekker, J.G., 1997. The primary production model in a
638 marine ecosystem model ERSEM II. Journal of Sea Research 38, 169–172.

639

640 Elser, J.J., Loladze, I., Peace, A.L., Kuang, Y., 2012. Lotka re-loaded: modelling trophic
641 interactions under stoichiometric constrains. Ecological Modelling 245, 3-11

642

643 Flynn, K.J., Davidson, K., Cunningham, A., 1996. Prey selection and rejection by
644 amicroflagellate; implications for the study and operation of microbial food webs. J. Exp.
645 Mar. Biol. Ecol. 196, 357-372

646

647 Flynn, K. J., Davidson, K., 1993. Predator–prey interactions between Isochrysis galbana and
648 Oxyrrhis marina. II. Release of non-protein amines and faeces during predation of Isochrysis.
649 J. Plankton Res., 15, 893–905.

650

651 Geider, R. J., MacIntyre, H. L., Kana, T. M., 1997. Dynamic model of phytoplankton growth
652 and acclimation: responses of the balanced growth rate and the chlorophyll a:carbon ratio to
653 light, nutrient-limitation and temperature. Mar. Ecol. Prog. Ser. 148, 187-200

654

655 Geider, R., La Roche, J., 2002. Redfield revisited: variability of C:N:P in marine microalgae
656 and its biochemical basis. European Journal of Phycology 37, 1-17

657

658 Hall, S.R., 2004. Stoichiometrically-explicit competition between grazers: species
659 replacement, coexistence, and priority effects along resource supply gradients. American
660 Naturalist 164, 157–172.

661

662 Huisman, J., van Oostveen, P., Weissing, F.J., 1999. Critical depth and critical turbulence:
663 Two different mechanisms for the development of phytoplankton blooms. Limnology and
664 Oceanography 44: 1781-1787

665

666 Hessen, O.D., Faerovig, J.P., Andersen, T., 2002. Light, nutrients, and P:C ratios in algae:
667 grazer performance related to food quality and quantity. Ecology 83, 1886-1898

668

669 Irigoien, X., Flynn K.J., Harris, R.P., 2005. Phytoplankton blooms: a 'loophole' in
670 microzooplankton grazing impact? J. Plankton Res. 27, 313-321

671

672 Jones, R.H, Flynn, K.J., 2005. Nutritional status and diet composition affect the value of
673 diatoms as copepod prey. Science 307, 1457-14-59

674

675 Kiørboe, T., 2008. A mechanistic approach to plankton ecology. Princeton University Press,
676 209 pp

677

678 Kondo, J., 1975. Air-sea bulk transfer coefficients in adiabatic conditions. Boundary-Layer
679 Meteorol., 9, 91–112.

680

681 Kovala, P. E., Larrance, J. D., 1966. Computation of phytoplankton cell numbers, cell
682 volume, cell surface and plasma volume per liter, from microscopical counts. DTIC
683 Document.

684

685 Legendre, L., 1990. The significance of microalgal blooms for fisheries and for the export of
686 particulate organic carbon in oceans. J. Plankton Res. 12, 681-699

687

688 Loladze, I., Kuang, Y., Elser, J.J., 2000. Stoichiometry in producer-Grazer System: linking
689 Energy Flow with Elemental Cycling. *Bulletin of Mathematical Biology*, 62: 1137-1162.

690

691 Loladze, I., Kuang, Y., Elser, J.J., Fagan, W.F., 2004. Competition and stoichiometry:
692 coexistence of two predators on one prey. Journal of Theoretical Biology 65, 1–15
693

694

695 Martiny, A. C., Vrugt, J.A., Primeau, F.W., Lomas M.W., 2013. Regional variation in the
696 particulate organic carbon to nitrogen ratio in the surface ocean. Global Biogeochem. Cycles,
697 27, 723–731, doi:10.1002/gbc.20061.

698

699 Menden-Deuer, S., Lessard, E. J., 2000. Carbon to volume relationships for dinoflagellates,
700 diatoms, and other protist plankton. Limnology and oceanography, 45, 569-579.

701

702 Mitra, A., 2006. A multi-nutrient model for the description of the stoichiometric modulation
703 of predation in micro- and mesozooplankton. J. Plankton. Res. 28, 597-611

704

705 Mitra, A., Flynn, K.J., 2006. Promotion of harmful algal blooms by zooplankton predatory
706 activity. Biology Letters 2, 294-197

707

Mitra, A, Flynn, K.J., 2007. Effects of food quality and quantity on consumer gut passage time; impacts on predation kinetics and trophic dynamics. Am. Nat. 169:632-646.

Mitra, A., Castellani, C., Gentleman, W., Jónasdóttir, S.H., Flynn, K.J., Bode, A., Halsband, C., Kuhn, P., Licandro, P., Agersted, M.D., Calbet, A., Lindeque, P., Koppelmann, R., Møller, E.F., Gislason, A., Nielsen, T.G., St. John, M., 2014. Bridging the gap between marine biogeochemical and fisheries sciences; configuring the zooplankton link. Prog. Oceanogr., in press. http://dx.doi.org/10.1016/j.pocean.2014.04.025.

Pastres, R., Ciavatta, S., 2005. A comparison between the uncertainties in model parameters and in forcing functions: its application to a 3D water-quality model. *Environmental Modelling & Software*, *20*(8), 981-989.

Polimene, L., Brunet, C., Butenschon, Martinez-Vicente, V., M., Widdicombe, C., Torres, R., Allen, J.I.,. 2014. Modelling a light-driven phytoplankton succession. J. Plankton Res. 36, 214-229

Polovina, J. J., Howell, E. A., Abecassis, M., 2008. Ocean's least productive waters are expanding, Geophys. Res. Lett., 35, L03618, doi:10.1029/2007GL031745.

Rosati, A., Miyakoda, K., 1988. A general circulation model for upper ocean simulation. J. Phys. Oceanogr., 18, 1601–1626.

Sailley, S.F., Vogt, M., Doney, S.C., Aita, M.N., Bopp, L., Buitenhuis, E.T., Hashioka, T., Lima, I., Le Quere, C., Yamanaka, Y., 2013. Comparing food web structures and dynamics across a suite of marine ecosystem models. Ecological Modelling. 261-262, 43-57

Saltelli, A., K. Chan, and M. Scott (Eds.) (2000). *Sensitivity Analysis*. Wiley Series in Probability and Statistics. New York: John Wiley and Sons.

Sarmiento, J.L., Gruber, N., 2006. Ocean Biogeochemical Dynamics. Princeton University Press

741 Siuda, N.S.A., Dam, G.H., 2010. Effects of omnivory and predator-prey elemental
742 stoichiometry on planktonic trophic interactions. Limnol. Oceanogr. 55, 2107-2116
743
744 Smyth, T. J., Fishwick, J. R., Al-Moosawi, L., Cummings, D.G., Harris, C., Kitidis, V., Rees,
745 A., Martinez-Vicente, V., Woodwaed, E.M.S., 2010. L4 in context: a broad spatio-temporal
746 view in the Western English Channel Observatory. J. Plankton Res., **32**, 585–601
747
748 Smyth, T.J., Allen, I., Atkinson, A., Bruun, J.T., Harmer, R.A., Pingree, R.D., Widdicombe
749 C.E., Somerfield, P.J., 2014. Ocean Net Heat Flux Influences Seasonal to Interannual
750 Patterns of Plankton Abundance. PLoS ONE 9(6): e98709.
751 doi:10.1371/journal.pone.0098709
752
753 Stiefs, D., van Voorn, G.A.K., Kooi, B.W., Feudel, U., Gross, T., 2010. Food quality in
754 producer–grazer models: a generalized analysis. American Naturalist, 176367–176380.
755
756 Taylor, J.R., Ferrari, R., 2011. Shutdown of turbulent convection as a new criterion for the
757 onset of springphytoplankton blooms. Limnology and Oceanography 56: 2293-2307.
758
759 Urabe, J., Sterner, W.R., 1996. Regulation of herbivore growth by the balance of light and
760 nutrients. Proc. Natl. Acad. Sci. 93, 8465-8469
761
762 Vichi, M., Masina, M.,Pinardi, N., 2007. A generalized model of pelagic biogeochemistry for
763 the global ocean ecosystem. Part I: Theory. J. Mar. Sys. 64, 89–109.
764
765 Widdicombe, C.E., Eloire, D., Harbour, D. Harris, R.P., Somerfield, P.J., 2010. Long-term
766 phytoplankton community dynamics in the Western English Channel. J.Plankton Res. 32,
767 643-655.
768
769 Woodward, E.M.S., Harris, C., Al-Moosawi, L., 2013. Nutrient concentration profiles from
770 long term time series at Station L4 in the Western English Channel from 2000 to 2012.
771 British Oceanographic Data Centre - Natural Environment Research Council UK.
772 doi:10.5285/075f8000-7114-11e2-907f-1803734a77fb
773
774

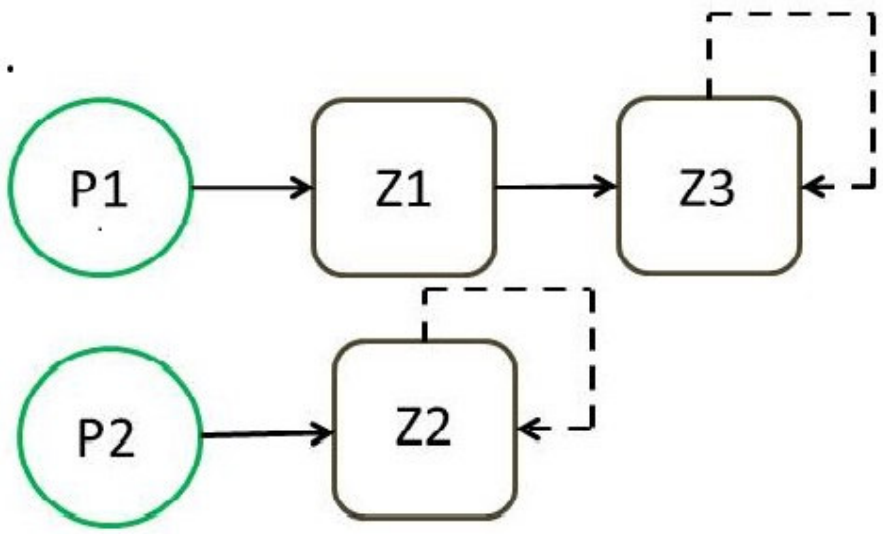

775

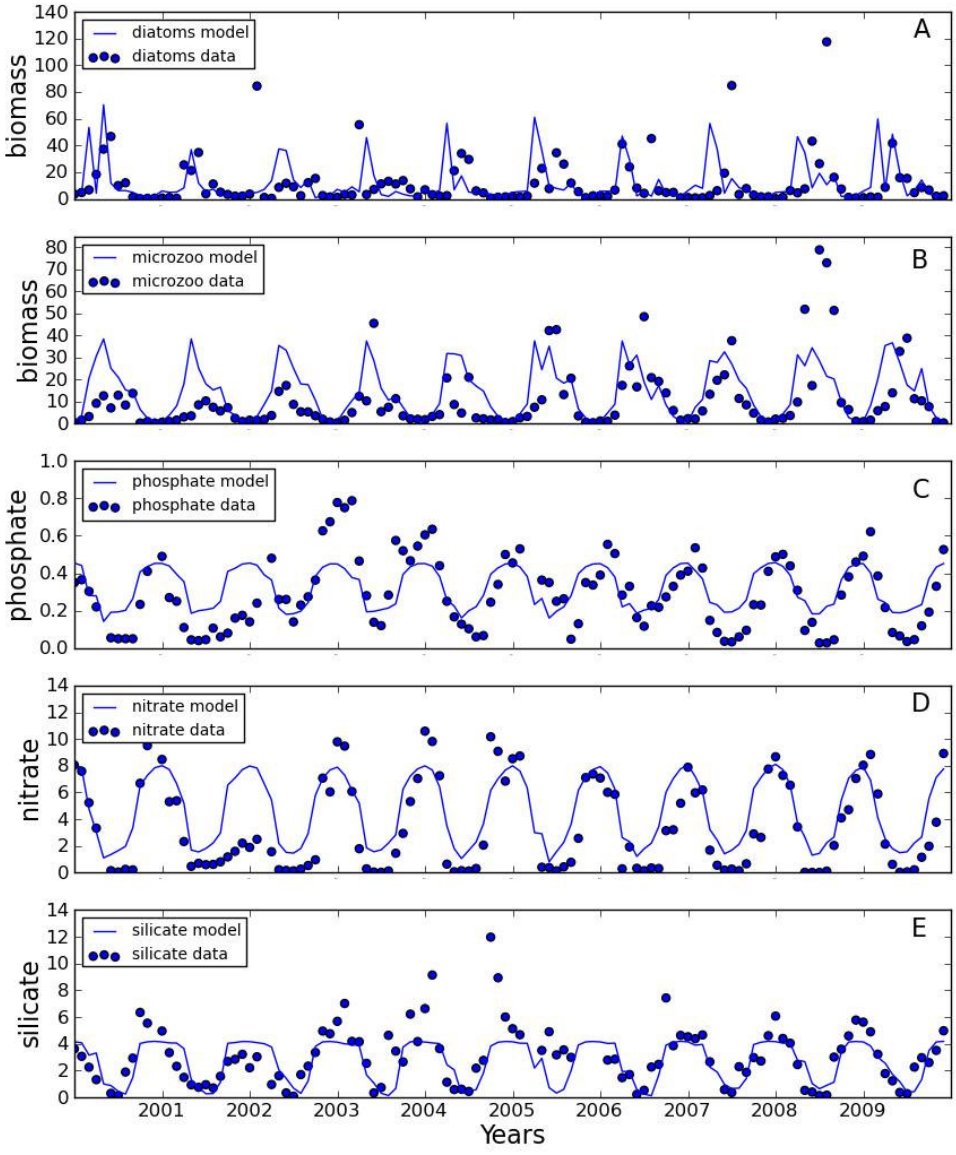

776

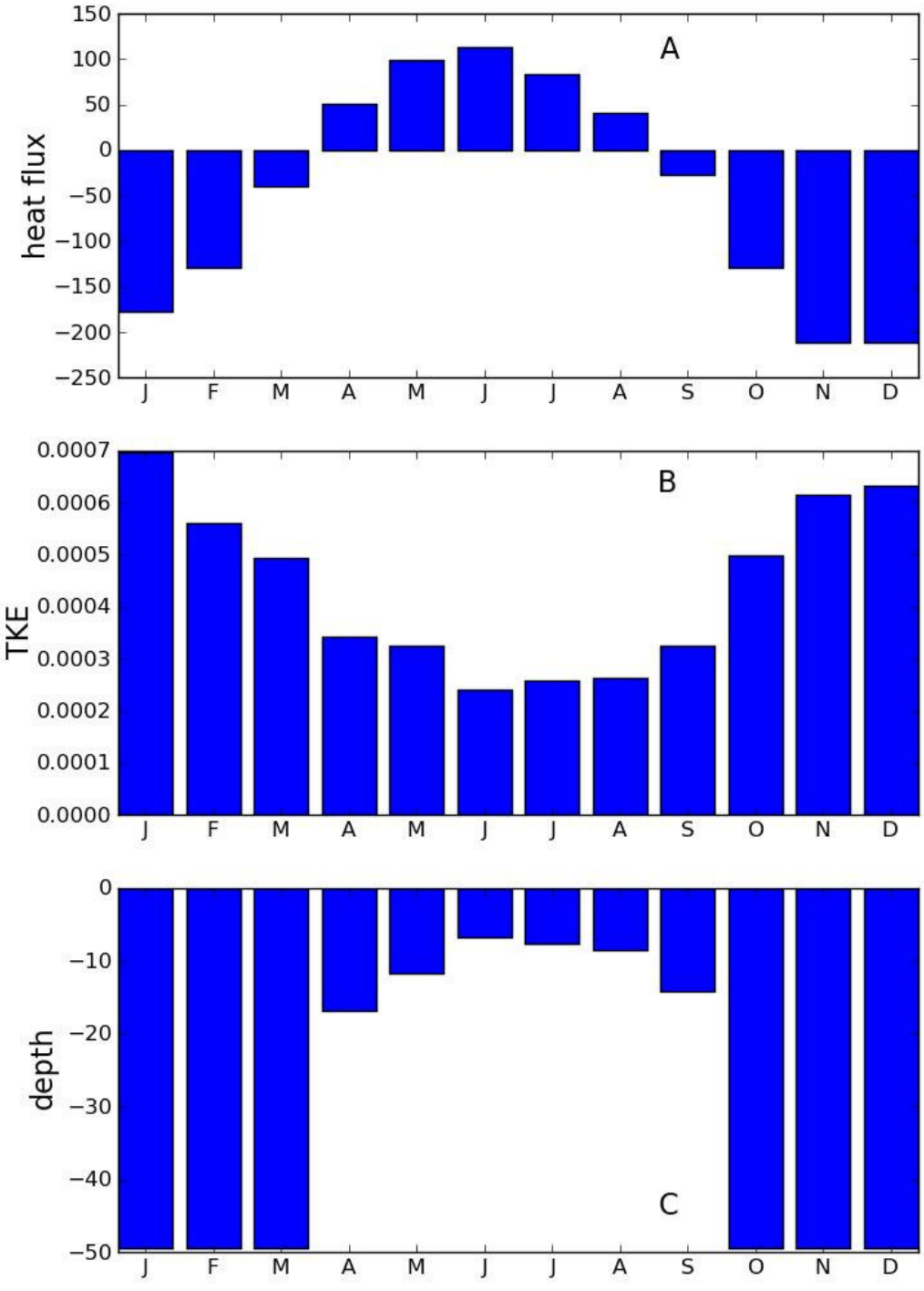

777

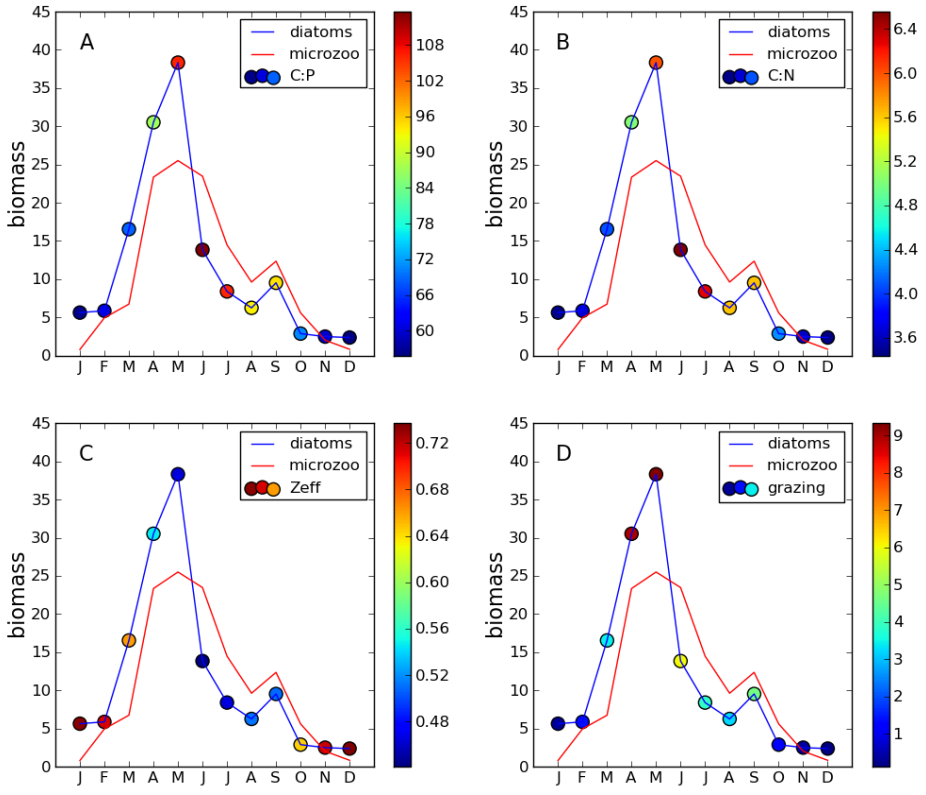

778

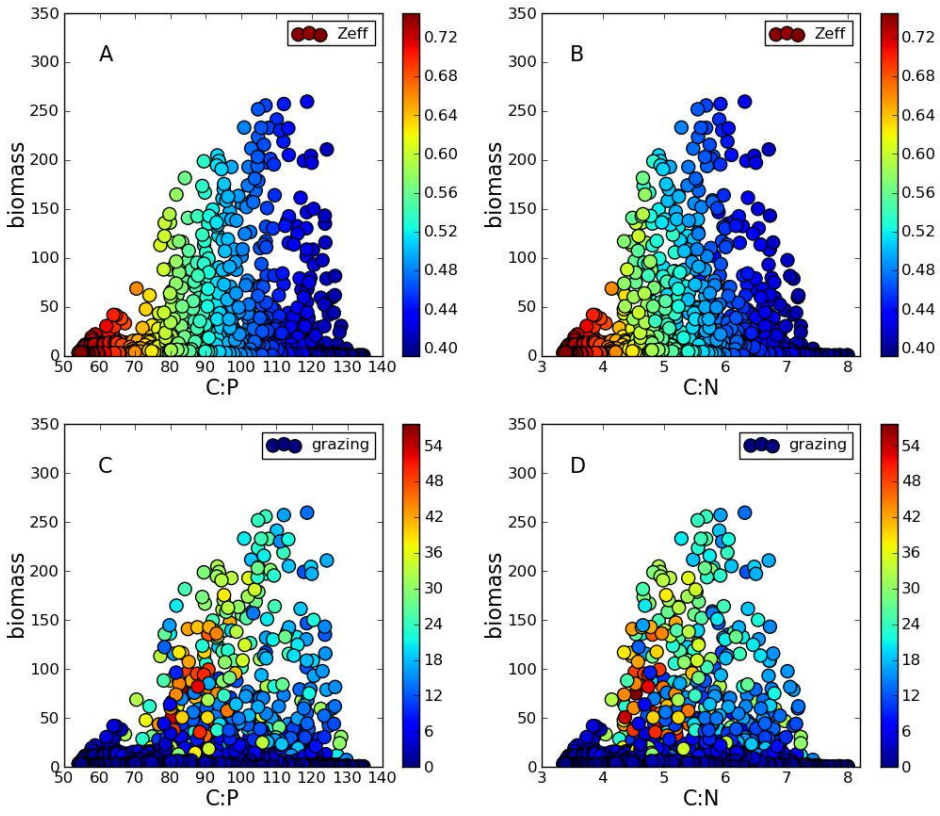

779

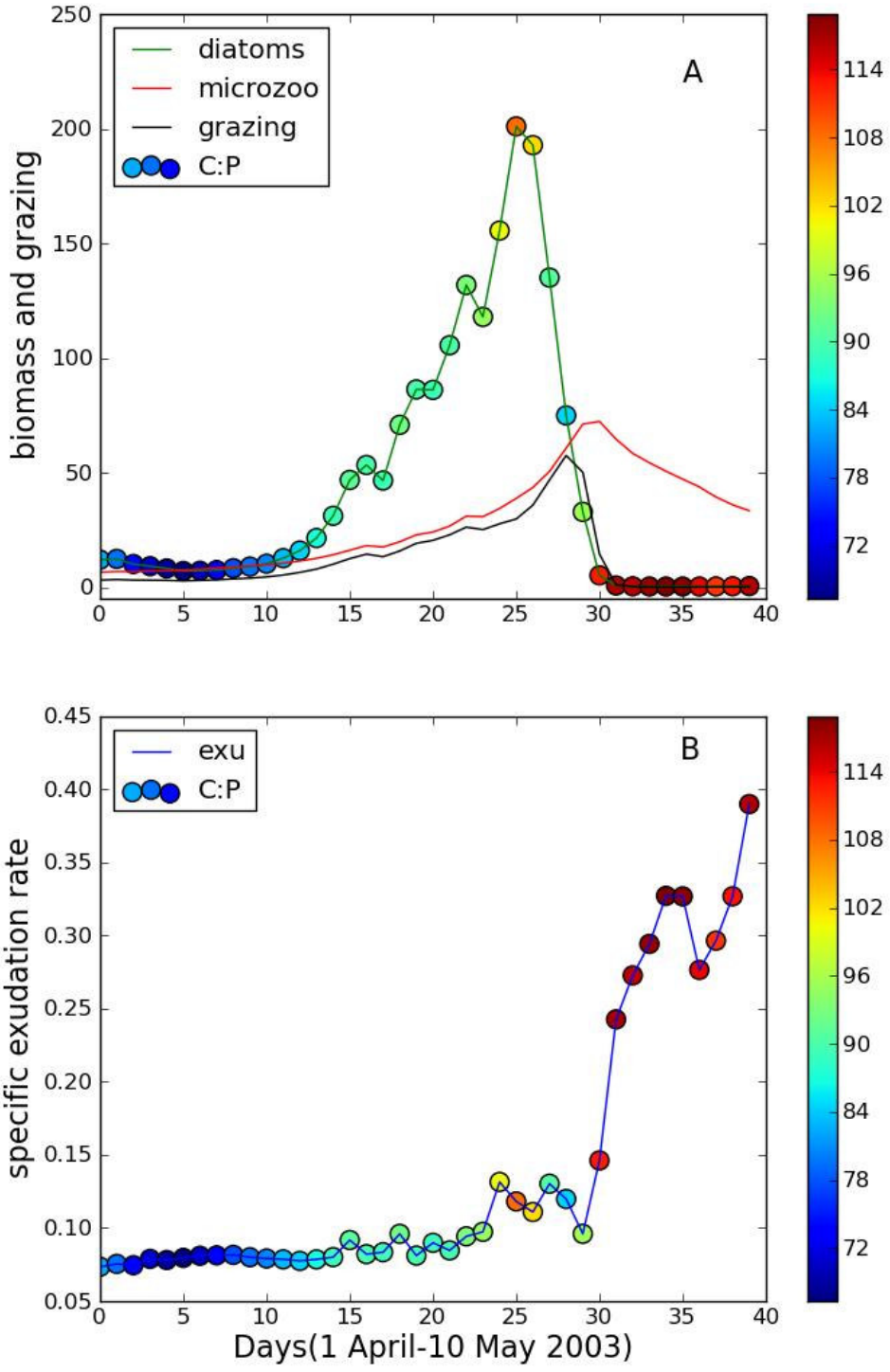

780

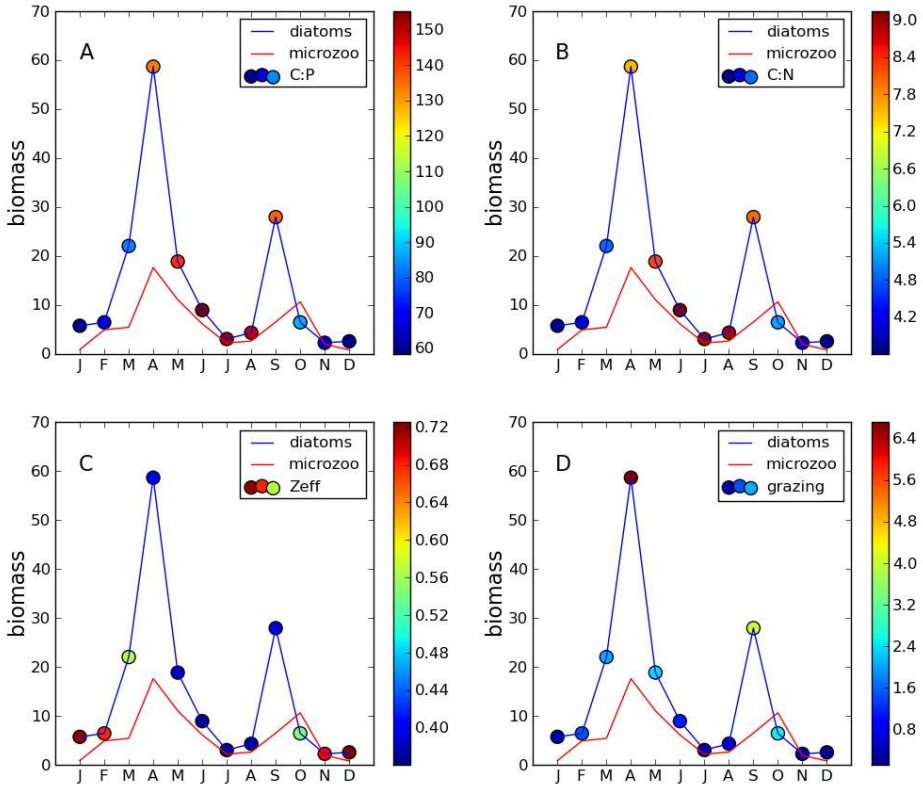

781

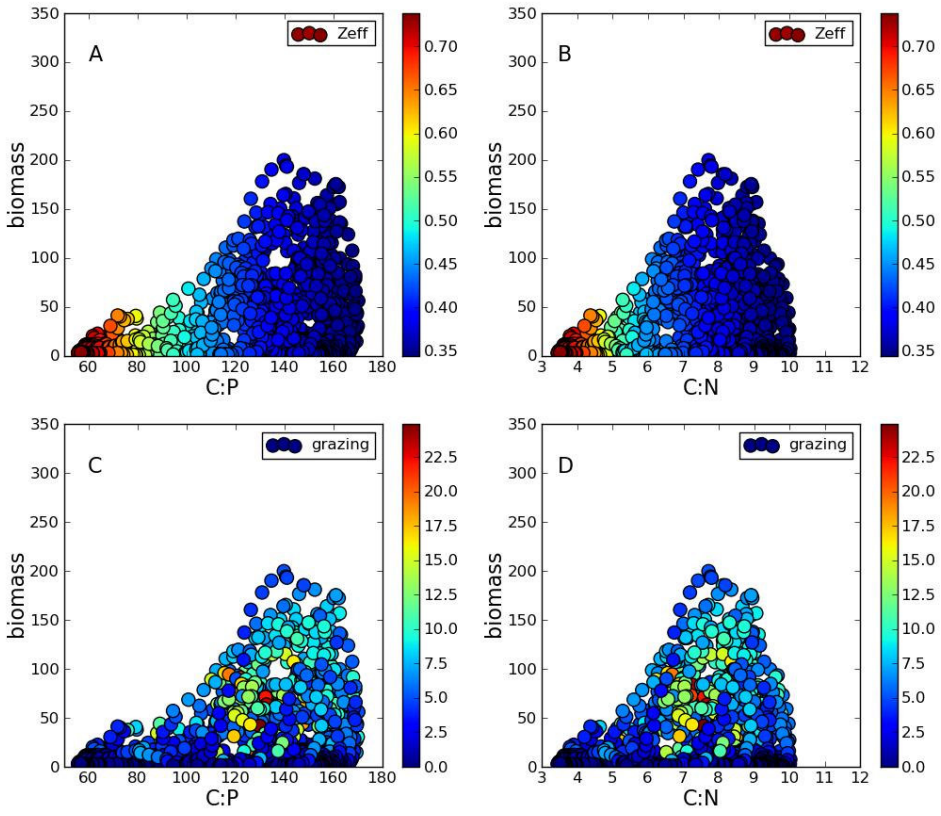

782

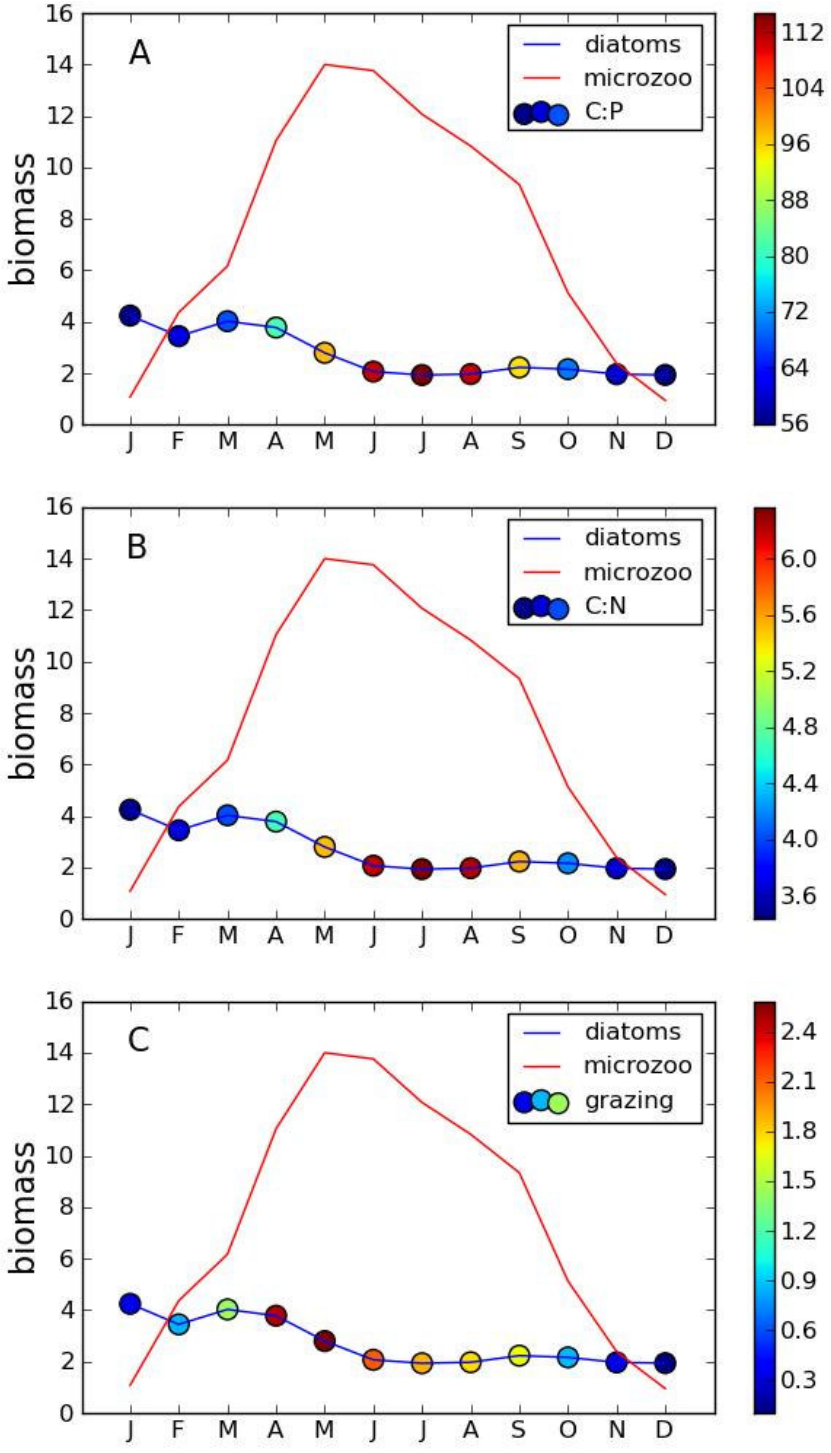

783

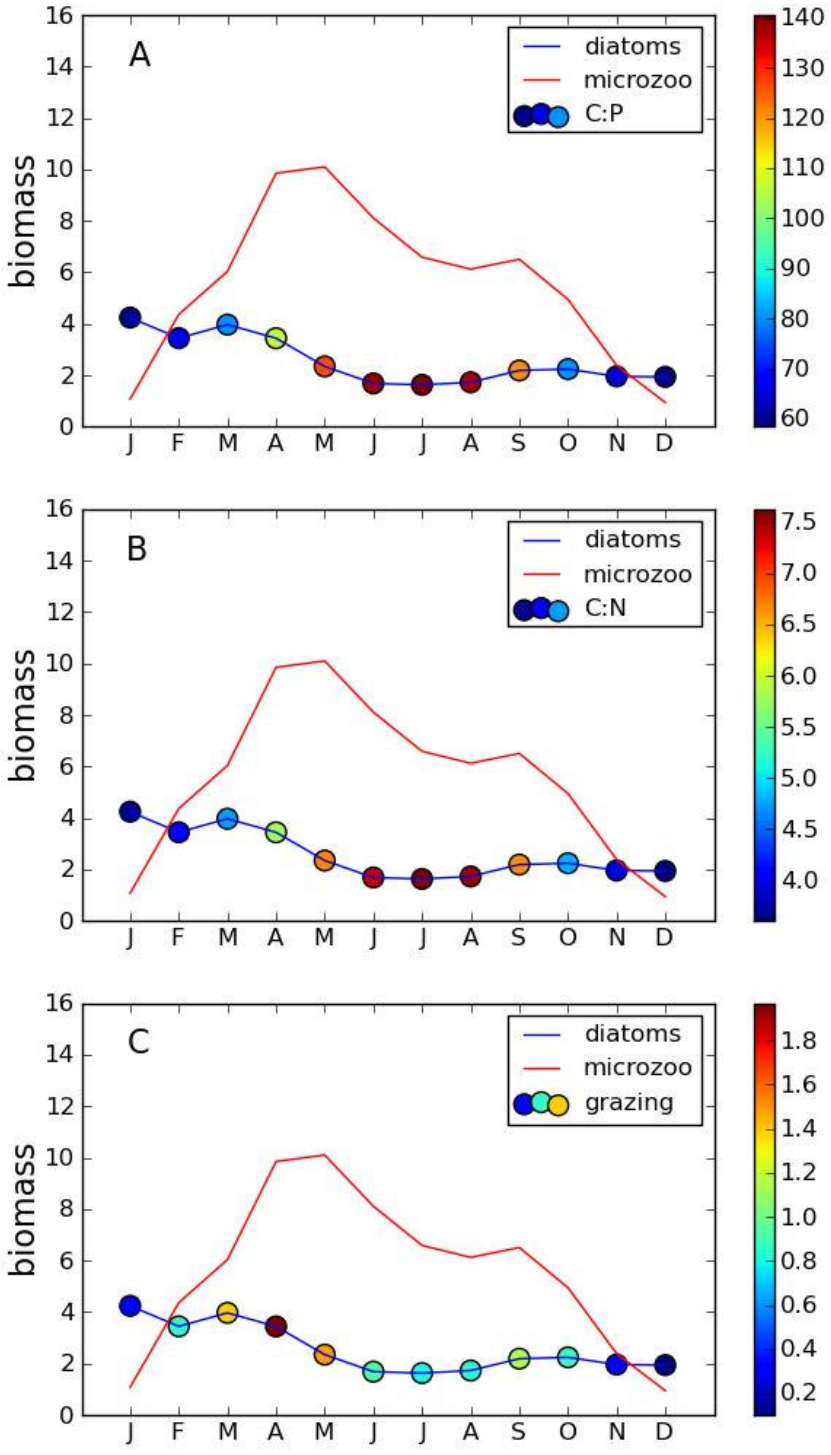

784

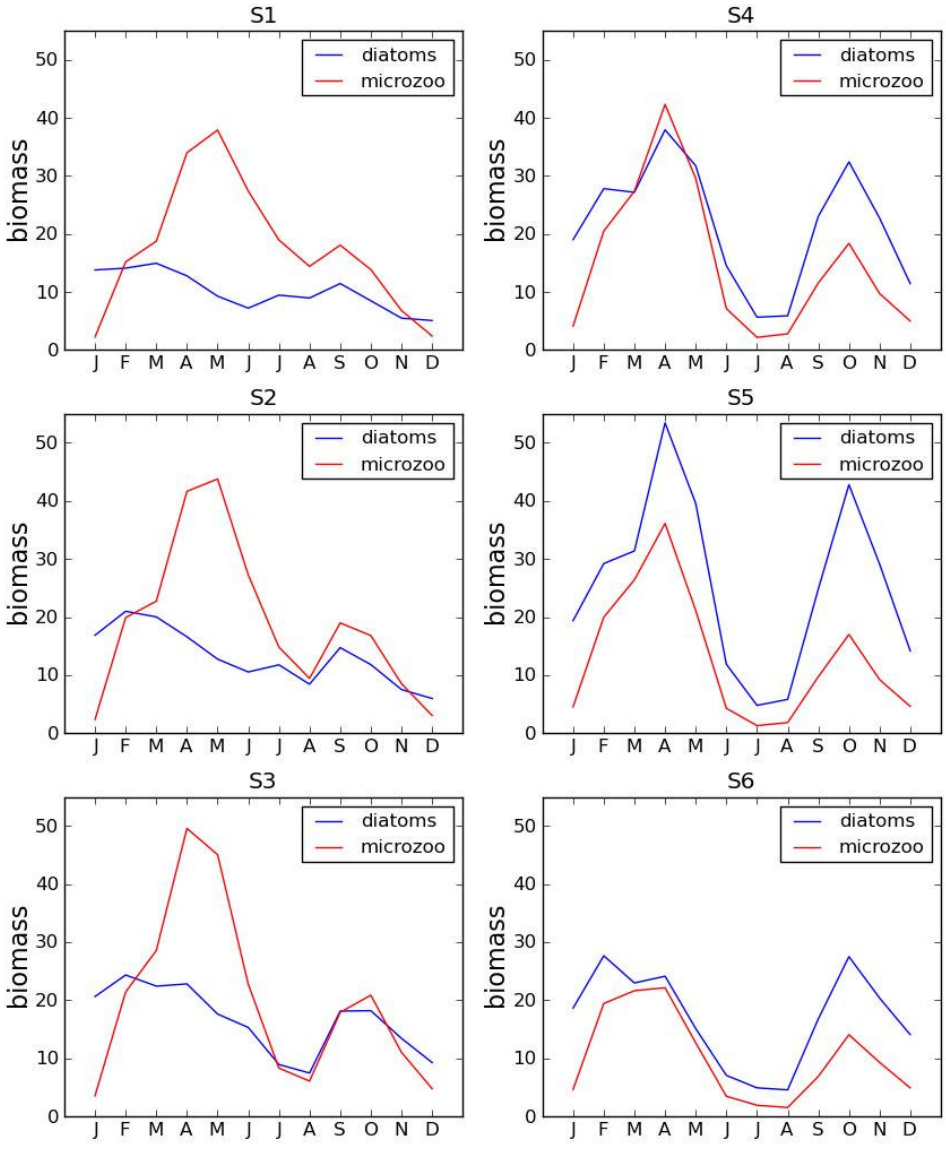

785

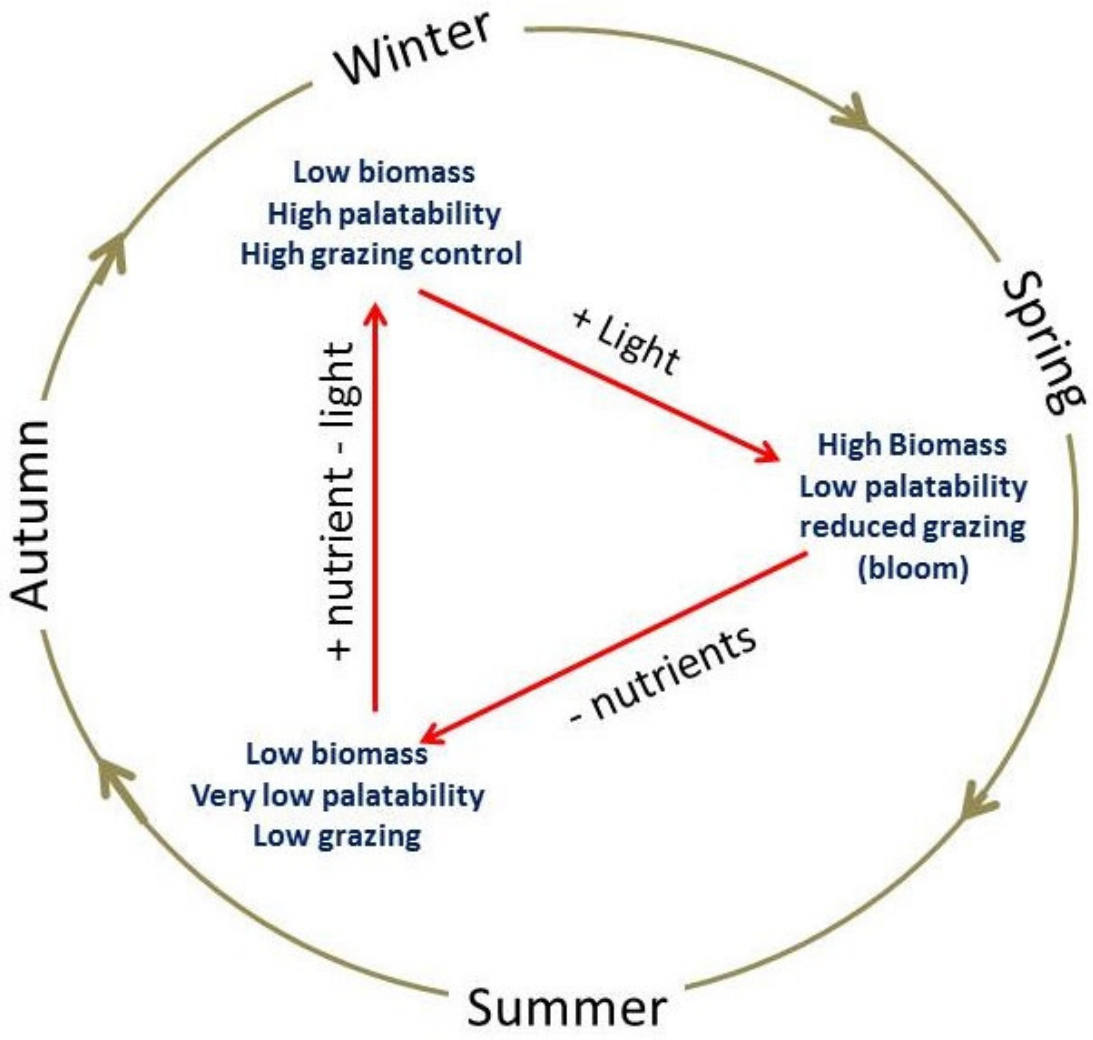
Winter
Spring
Summer
Autumn
Low biomass
High palatability
High grazing control
+ Light
High Biomass
Low palatability
reduced grazing
(bloom)
- nutrients
Low biomass
Very low palatability
Low grazing
+ nutrient - light

786

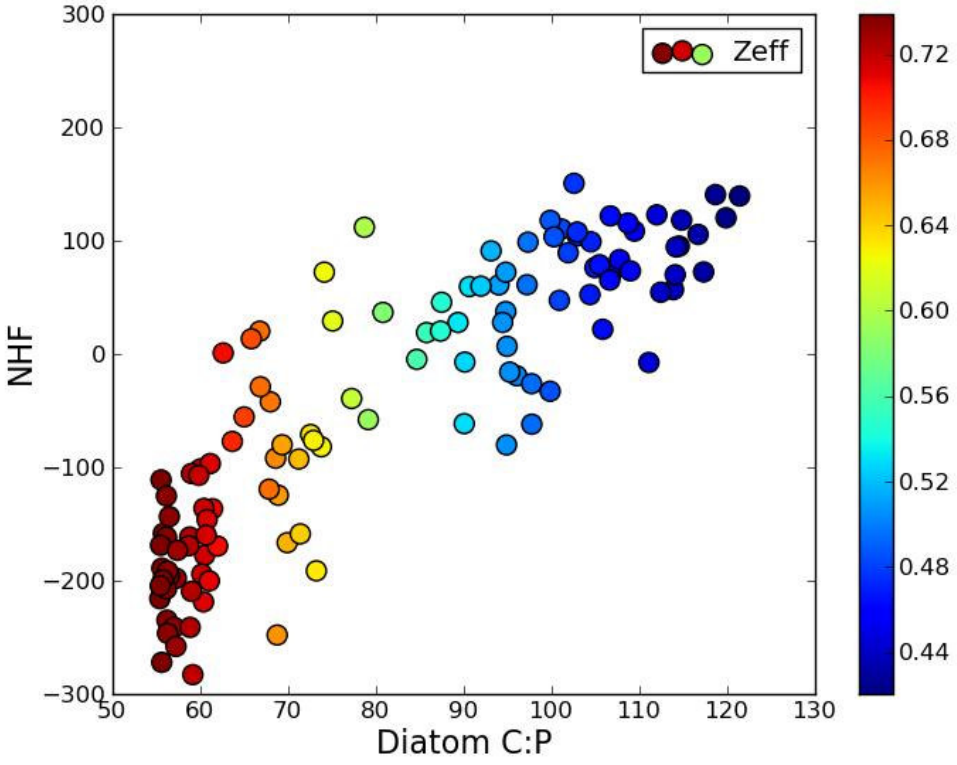

787

788

789

790

791 Highlights

792 • Abiotic and biotic mechanisms underpin bloom dynamics
793 • Phytoplankton nutritional status contributes to bloom formation and evolution
794 • High C:P in diatoms reduces the transfer of carbon to the higher trophic levels.

795

796